

## Use of in situ cloud condensation nuclei, extinction, and aerosol size distribution measurements to test a method for retrieving cloud condensation nuclei profiles from surface measurements

Steven J. Ghan,<sup>1</sup> Tracey A. Rissman,<sup>2</sup> Robert Elleman,<sup>3</sup> Richard A. Ferrare,<sup>4</sup> David Turner,<sup>1</sup> Connor Flynn,<sup>1</sup> Jian Wang,<sup>5</sup> John Ogren,<sup>6</sup> James Hudson,<sup>7</sup> Hafliði H. Jonsson,<sup>8</sup> Timothy VanReken,<sup>2</sup> Richard C. Flagan,<sup>2</sup> and John H. Seinfeld<sup>2</sup>

Received 28 December 2004; revised 21 April 2005; accepted 19 July 2005; published 19 January 2006.

[1] If the aerosol composition and size distribution below cloud are uniform, the vertical profile of cloud condensation nuclei concentration can be retrieved entirely from surface measurements of CCN concentration and particle humidification function and surface-based retrievals of relative humidity and aerosol extinction or backscatter. This provides the potential for long-term measurements of CCN concentrations near cloud base. We have used a combination of aircraft, surface in situ, and surface remote sensing measurements to test various aspects of the retrieval scheme. Our analysis leads us to the following conclusions. The retrieval works better for supersaturations of 0.1% than for 1% because CCN concentrations at 0.1% are controlled by the same particles that control extinction and backscatter. If in situ measurements of extinction are used, the retrieval explains a majority of the CCN variance at high supersaturation for at least two and perhaps five of the eight flights examined. The retrieval of the vertical profile of the humidification factor is not the major limitation of the CCN retrieval scheme. Vertical structure in the aerosol size distribution and composition is the dominant source of error in the CCN retrieval, but this vertical structure is difficult to measure from remote sensing at visible wavelengths.

**Citation:** Ghan, S. J., et al. (2006), Use of in situ cloud condensation nuclei, extinction, and aerosol size distribution measurements to test a method for retrieving cloud condensation nuclei profiles from surface measurements, *J. Geophys. Res.*, *111*, D05S10, doi:10.1029/2004JD005752.

### 1. Introduction

[2] One of the greatest sources of uncertainty in estimates of global climate change by climate models is in the treatment of indirect effects of aerosols on cloud optical depth through the role of aerosols as cloud condensation nuclei (CCN). All cloud droplets form on aerosol particles, so the CCN concentration has a powerful influence on droplet number concentration. However, the maximum supersaturation (which largely determines the number of CCN activated) in updrafts depends on the updraft velocity, which is highly variable within the droplet nucleation zone of clouds. Furthermore, droplet number is reduced by

evaporation, by droplet collision and coalescence with other droplets and with precipitating drops, and the precipitation process (which reduces the liquid water path of the cloud) which depends on both the mean and the dispersion of the droplet number size distribution [Liu and Daum, 2002].

[3] These complicating factors make it very difficult to represent aerosol indirect effects in climate models, to evaluate that representation, and to isolate the aerosol indirect effect from field measurements. Aircraft measurements have been used to evaluate droplet nucleation models [Lin and Leaitch, 1997; Gultepe et al., 1998; Yum and Hudson, 2002; Hudson and Yum, 2002; Snider et al., 2003; Conant et al., 2004; Peng et al., 2005], but such high-quality measurements are too costly to permit the collection of the thousands of independent samples needed to isolate the indirect effect in models and observations. Moreover, they do not permit the simultaneous measurement of cloud base properties (updraft velocity and CCN concentration) and column integrated properties (liquid water path and optical depth). Satellite retrievals provide a large sample size of measurements of column integrated properties [Han et al., 1998], but cannot provide estimates of updraft velocity and CCN concentration at cloud base. Surface in situ measurements on mountaintops [Hallberg et al., 1997; Menon and Saxena, 1998; Menon et al., 2002] provide an

<sup>1</sup>Pacific Northwest National Laboratory, Richland, Washington, USA.

<sup>2</sup>California Institute of Technology, Pasadena, California, USA.

<sup>3</sup>Department of Atmospheric Science, University of Washington, Seattle, Washington, USA.

<sup>4</sup>NASA Langley Research Center, Hampton, Virginia, USA.

<sup>5</sup>Brookhaven National Laboratory, Upton, New York, USA.

<sup>6</sup>NOAA Climate Monitoring and Diagnostics Laboratory, Boulder, Colorado, USA.

<sup>7</sup>Desert Research Institute, Reno, Nevada, USA.

<sup>8</sup>Naval Postgraduate School, Monterey, California, USA.

economical source of measurements but are only useful when cloud base is near the elevation of the site. Consequently, there have been few attempts to use measured CCN concentration to evaluate the treatment of indirect effects in climate models [Menon *et al.*, 2003; Ovtchinnikov and Ghan, 2005].

[4] Surface-based remote sensing offers some appealing advantages to these other measurement strategies. By looking upward from the surface, profilers can provide useful information about the aerosol up to cloud base, about updrafts within the cloud, and about column-integrated cloud properties such as liquid water path and cloud optical depth. This permits long-term collection of data that can be used to isolate the aerosol indirect effect and evaluate the treatment of it in single column versions of global climate models.

[5] Kim *et al.* [2003] and Penner *et al.* [2004] used surface-based remote sensing of cloud optical depth and liquid water path to demonstrate how the dependence of optical depth on liquid water path (i.e., the droplet effective radius) varies from day to day, but only used a surface measure of the aerosol to relate to this dependence. Feingold *et al.* [2003] extended this method by relating the droplet effective radius to the aerosol extinction near cloud base.

[6] Although aerosol extinction might serve as a first approximation to CCN concentration, further improvements are possible by (1) accounting for the influence of water uptake on extinction and (2) using the resulting dry extinction to scale surface measurements of CCN concentration. This provides the ability to estimate the full CCN spectrum at cloud base, if the spectrum is measured at the surface.

[7] This method for estimating CCN concentration near cloud base was suggested by Ghan and Collins [2004, hereinafter referred to as GC]. In this retrieval, surface measurements of the CCN concentration  $CCN(S, z_0)$  at supersaturation  $S$  are scaled by the ratio of the dry extinction (or  $180^\circ$  backscatter) profile  $\sigma_{de}(z)$  to the dry extinction (or  $180^\circ$  backscatter) at or near the surface,  $\sigma_{de}(z_0)$ :

$$CCN(S, z) = CCN(S, z_0) \sigma_{de}(z) / \sigma_{de}(z_0) \quad (1)$$

The dry extinction (or  $180^\circ$  backscatter) profile  $\sigma_{de}(z)$  is determined from the extinction (or  $180^\circ$  backscatter) profile at ambient humidity  $\sigma_e(z)$  and the dependence of extinction (or  $180^\circ$  backscatter) on relative humidity,  $f(RH(z))$ :

$$\sigma_{de}(z) = \sigma_e(z) / f(RH(z)) \quad (2)$$

The aerosol particle humidification factor  $f(RH)$  is measured at the surface and is assumed to apply at all levels up to cloud base using the retrieved relative humidity profile. GC describe the instruments that can be used to provide the necessary measurements for this retrieval. Anderson *et al.* [2000] and GC show that for  $RH$  up to 80%,  $f(RH)$  for extinction is indistinguishable from  $f(RH)$  for  $180^\circ$  backscatter. We will therefore use the same expression for both.

[8] The method assumes the humidification factor measured at the surface is representative of the humidification factor at altitude, and it assumes that the vertical structure of CCN concentration is identical to the vertical structure of dry extinction or backscatter. Since both extinction/

backscatter and CCN concentration are determined entirely by the size distribution of aerosol number, composition, and geometric shape, both of these assumptions are valid if (1) the aerosol size distribution (but not necessarily the total aerosol number) is independent of altitude, and (2) the aerosol composition and particle shape are independent of altitude. GC used in situ aerosol size distribution measurements, Mie theory, and Köhler theory to examine the vertical variability of the size distribution, but did not have the CCN or aerosol composition measurements needed to investigate the vertical variability of aerosol composition and shape. Clearly the impact of this variability on the retrieval also needs to be tested.

[9] In May 2003 the Atmospheric Radiation Measurement (ARM) program conducted an aerosol intensive observation period (IOP) that provides the data needed to test assumptions A and B. The goal of this study is to evaluate the GC CCN retrieval and to understand what is limiting its performance. In section 2 we describe the design of the ARM experiment, and in section 3 we describe the use of the measurements to evaluate the performance of the retrieval scheme. Conclusions are summarized in section 4.

## 2. Experiment Design

### 2.1. Instruments and Measurements

[10] To distinguish between different sources of error in the retrieval scheme, a variety of measurements were collected. These include both in situ and remote sensing measurements. In situ measurements were collected both from aircraft and at the surface.

#### 2.1.1. Measurements From Aircraft

[11] In situ measurements include (1) CCN concentration, (2) aerosol size distribution, (3) relative humidity, (4) aerosol scattering and absorption, and (5) aerosol particle humidification factor. Although in situ measurements of aerosol composition and shape are not available (except for composition at the ground), the measurements of CCN concentration, aerosol scattering and absorption, and humidification provide the opportunity to test the influence of variability in aerosol composition and shape on the CCN retrieval because each of these fields depend on aerosol composition and shape.

[12] The CCN concentrations were measured from the Center for Interdisciplinary Remotely Piloted Aircraft Studies (CIRPAS) Twin Otter aircraft every second by the California Institute of Technology (Caltech) CCN counter. The CCN counter has three columns, each operating with a linear axial temperature gradient, allowing each column to achieve one supersaturation. Only two of the columns operated during the IOP. Because of undetected problems with the detector on column 2, the supersaturation for column 2 could not be determined for any of the flights, so the CCN concentrations for column 2 will not be considered here. The operating supersaturation of column 1 was determined from the critical supersaturation of  $(\text{NH}_4)_2\text{SO}_4$  particles with dry size such that 50% of a controlled size are able to activate in the CCN counter. The Köhler theory [Brechtel and Kreidenweis, 2000a, 2000b] is used to determine the critical supersaturation as a function of dry size (activation diameter  $d_{pc}$ ), and a differential mobility analyzer (DMA) is used to select a

**Table 1.** Flight Summary With Operating Conditions for CCNC3 Column 1

Flight Number	Date	Flight Begin Time, UTC	Flight End Time, UTC	Flight Length, hours	Activation Diameter, nm	Operating Supersaturation, %
6	14 May	1553	2019	4.4	15 ± 0.8	2.8 ± 0.2
7	14 May	2124	2248	1.4	15 ± 0.8	2.8 ± 0.2
8	15 May	1634	1909	2.6	15 ± 0.8	2.8 ± 0.2
9	17 May	1402	1805	4.0	13 ± 0.6	3.6 ± 0.4
10	18 May	1543	1745	2.0	15 ± 0.8	2.8 ± 0.2
12	21 May	1551	1847	2.9	18 ± 0.9	2.1 ± 0.2
13	22 May	1325	1813	4.8	18 ± 0.9	2.1 ± 0.2
14	25 May	1852	2212	3.3	18 ± 0.9	2.1 ± 0.2
15	27 May	1420	1929	5.2	18 ± 0.9	2.1 ± 0.2
16	28 May	1824	2205	3.7	18 ± 0.9	2.1 ± 0.2
17	29 May	1411	1751	3.7	18 ± 0.9	2.1 ± 0.2

variety of dry diameters which are then split to the CCN counter and a TSI Model 3010 condensation particle counter. Droplet density is calculated from Tang's polynomials [Tang and Munkelwitz, 1994]; the full Pitzer model [Pitzer, 1973; Pitzer and Mayorga, 1973] is used to calculate the osmotic coefficient; surface tension values from Pruppacher and Klett [1997] are used for surface tension. The calibrated activation diameters and the operating supersaturations for Column 1 are given in the legend in Table 1.

[13] The supersaturations listed in Table 1 are quite high, all above 2%. Such high supersaturations are typically expected only for strong updrafts and clean conditions. Moreover, unless particles have high insoluble contents, most of the particles that can be activated at such high supersaturations are usually quite small, with radius between 20 and 100 nm (although larger particles are also activated, their number concentrations are usually much smaller than those of particles smaller than 100 nm radius). These particles have little impact on extinction or backscatter, which are most sensitive to particles with radius between 100 and 600 nm [Ghan and Collins, 2004]. Thus extinction and backscatter will be well correlated with CCN concentration at such supersaturations only if the particles have high insoluble contents or if the aerosol size distribution varies little with altitude so that the concentration of particles with radii between 20 and 100 nm varies in concert with the concentration of particles with radii between 100 and 600 nm. These in situ CCN measurements therefore provide a difficult test of the CCN retrieval scheme. CCN concentration at lower supersaturations, which is dominated by larger particles that produce stronger extinction and backscatter signatures, should be more accurately retrieved by the scheme.

[14] The aerosol size distribution was measured at 72.5 s intervals at ambient relative humidity by a Caltech DMA [Wang et al., 2003]. Particles were dried to below 25% RH prior to measurements. The sizes are centered at 23 diameters ranging from 19 to 620 nm.

[15] Relative humidity is calculated from the ambient temperature (calculated from Rosemount total temperature and true airspeed) and dew point temperature (measured by Edgetech EG&G chilled mirror).

[16] Aerosol scattering at wavelengths of 450, 550, and 700 nm was measured every 8 s by a TSI model 3563 nephelometer for dry conditions. The data have been corrected for nonidealities and corrected to ambient temperature and pressure [Anderson and Ogren, 1998]. Aerosol absorption at wavelengths of 467, 530, and 660 nm is

measured by a Particle Soot Absorption Photometer (PSAP). The scattering data have been adjusted to the PSAP wavelengths using the Ångström exponent. Unrealistic data points due to instrument malfunction, adjustment in flight, and data acquisition problems have been removed from all data sets.

[17] The humidification factor at a wavelength of 540 nm is approximated by

$$f(RH) = \left( \frac{1 - RH_{lo}}{1 - RH} \right)^\gamma \quad (3)$$

where  $\gamma$  is determined from a fit to humidograph scattering measurements at two different humidities:

$$\gamma = \frac{\ln(\sigma_{hi}/\sigma_{lo})}{\ln[(1 - RH_{lo})/(1 - RH_{hi})]} \quad (4)$$

where  $RH_{lo}$  and  $RH_{hi}$  are typically 30% and 80%, respectively.

### 2.1.2. Surface Measurements

[18] At the surface, both in situ and remote sensing measurements were collected at the ARM Climate Research Facility (CRF) central site near Lamont Oklahoma. Remote sensing measurements were provided by the CRF Raman lidar (CARL) and the micropulse lidar (MPL). CARL provides retrievals of both aerosol extinction and 180° backscatter at a wavelength of 355 nm [Ferrare et al., 2001; Turner et al., 2002], and relative humidity is estimated from the Raman lidar retrieval of absolute humidity and from a retrieval of temperature from an Atmospheric Emitted Radiance Interferometer (AERI). The Raman lidar retrievals are performed every 10 min and interpolated to a vertical resolution of 39 m. Comparisons of the CARL aerosol and water vapor profiles with these additional data sets acquired during the IOP as well as trends derived from long-term CARL measurements revealed several issues with the CARL data that adversely impacted retrievals of both aerosol and water vapor profiles. The sensitivity of the CARL had significantly declined since the end of 2001. This loss of sensitivity has greatly impacted the quality of the CARL aerosol backscattering and extinction profiles derived since this time and during the Aerosol IOP. Therefore the automated algorithms used to derive aerosol and water vapor profiles from the CARL data were modified in an attempt to reduce or remove these adverse effects. The extensive modifications made to the CARL automated

algorithms reduced but could not eliminate these adverse effects [Ferrare *et al.*, 2004, 2006]. Modifications and upgrades performed during 2004 have dramatically enhanced the sensitivity of CARL to surpass all previous performance levels [Turner and Goldsmith, 2005].

[19] The MPL provides vertical profiles of attenuated  $180^\circ$  backscatter every 30 s with 30 m vertical resolution. Current processing yields 10-min averaged profiles of aerosol extinction and  $180^\circ$  backscatter. However, in contrast to the Raman lidar technique, the MPL retrievals of extinction and backscatter are not truly independent, but are in fact related through an assumed constant extinction to backscatter ratio. This assumption will not always be valid, particularly in the case of separated aerosol layers. However, under well-mixed conditions the assumption typically has reasonable local validity.

[20] Schmid *et al.* [2006] compare in detail the Raman lidar and MPL retrievals of extinction with the in situ measurements collected during this IOP. We therefore will not compare the estimates here.

[21] Surface in situ measurements consisted of aerosol humidification and CCN spectra. Surface humidification measurements were provided by the Aerosol Observing System (AOS) humidograph system at the ARM Climate Research Facility [Sheridan *et al.*, 2001]. The same parametric representation for  $f(RH)$ , given by equation (3), is used. For consistency with the aircraft measurements, the humidification at 550 nm wavelength is used.

[22] CCN spectral measurements at the surface were provided by two Desert Research Institute CCN spectrometers [Hudson, 1989], which were operated over two different but overlapping supersaturation ranges. Concentrations at supersaturations between 0.03% and 1% are considered most accurate. The CCN concentrations were averaged over the period spanning the aircraft overflights. The time means will be used to scale the vertical distribution profile provided by dry extinction.

## 2.2. Platforms and Flight Patterns

[23] All airborne in situ measurements used in this study were collected from the CIRPAS Twin Otter, which has a cruising speed of about  $50 \text{ m s}^{-1}$ .

[24] The 2003 ARM aerosol IOP had a variety of objectives, but most required coincident in situ and remote sensing measurements of vertical profiles of aerosol and its microphysical and radiative properties. Thus, although a variety of aircraft flight patterns were employed on different days, useful data for testing the CCN retrieval scheme were collected on most flight days. Two flight patterns were most common: the spiral and the level legs. Spirals were typically performed with a 1 km diameter centered over the central site, with ascent/descent speeds of  $2\text{--}3 \text{ m s}^{-1}$ . Level legs were typically 15–30 km in length crossing over the central site, spaced every 500–1000 ft in altitude, with  $180^\circ$  turns between legs. All flight patterns were designed to prevent sampling of the aircraft's own exhaust.

## 2.3. Sampling

[25] Critical to the success of this study is the collocation of the aircraft and remote sensing measurements, both in space and time. To ensure this, samples were discarded unless all of the following conditions were met: (1) Aircraft

is within 30 km of SGP CF ( $36^\circ\text{N } 37' 97'' \text{ W } 30'$ ), (2) lidar samples at the same altitude as the aircraft and within 60 min of aircraft flyover, (3) cloud-free (number concentration of particles with diameter larger than  $2.5 \mu\text{m} < 10 \text{ cm}^{-3}$ ), (4) relative humidity  $<95\%$ , and (5) estimated error in extinction retrieved from Raman lidar  $<50\%$  of extinction. The 30 km and 60 min proximity criterion were determined from a compromise between the need to accumulate a sufficient number of samples and the need for collocation of in situ and remote sensing samples. We have found results to be insensitive to the spatial and temporal range of the sampling filter for distances between 5 and 30 km and time differences between 15 and 60 min. To permit comparison on a point-by-point basis, for each day the aircraft data were averaged over all the resulting samples within the 40 m thick lidar layers. This produces a single vertical profile of all fields for each day. However, values for many layers may not be defined, particularly for days without spiral flight patterns.

[26] To ensure a comparable evaluation of different retrievals, all quantities were sampled only when all sampling criteria were met. Although reliable in situ data were discarded, we felt it was more important to ensure a comparable evaluation than to have the most extensive sampling for each retrieval.

## 3. Analysis

[27] To evaluate the performance of the CCN retrieval scheme, we look at the data in three different ways. First we look at vertical profiles of normalized quantities to identify the vertical structure in the data and to see the relationships between different quantities. Then we use the full scheme to retrieve vertical profiles of CCN concentration. Finally, we look at vertical profiles of quantities that are sensitive to the size distribution and composition and hence can be used to determine whether the assumptions of the retrieval are valid.

### 3.1. Vertical Structure and Relationships

[28] The objective of this study is to determine how well the CCN retrieval scheme can determine the vertical profile of CCN concentration below cloud, and to understand what is limiting its performance. The measure of performance will be the agreement with in situ measurements of CCN concentration. To isolate errors due to differences between the CCN instruments on the ground and in the aircraft, we will compare vertical profiles of CCN concentration and dry extinction normalized by values at the lowest altitude available for all profiles. This still tests the validity of equation (1), but removes errors due to the very different designs and calibration procedures for the CCN instruments [Nenes *et al.*, 2001]. Errors in the measured variability of CCN (the gain) are not removed by normalization.

[29] Given the anchor point of the retrieval scheme at the surface, it is likely to perform well at altitudes near the surface. Such agreement is neither useful nor indicative of the performance of the retrieval scheme, because surface measurements without the scaling by dry extinction should provide close approximations to the CCN concentrations near the surface. We therefore have extended our evaluation up to 5 km above the surface. Although the performance of the scheme is likely to be worse far from the surface, such

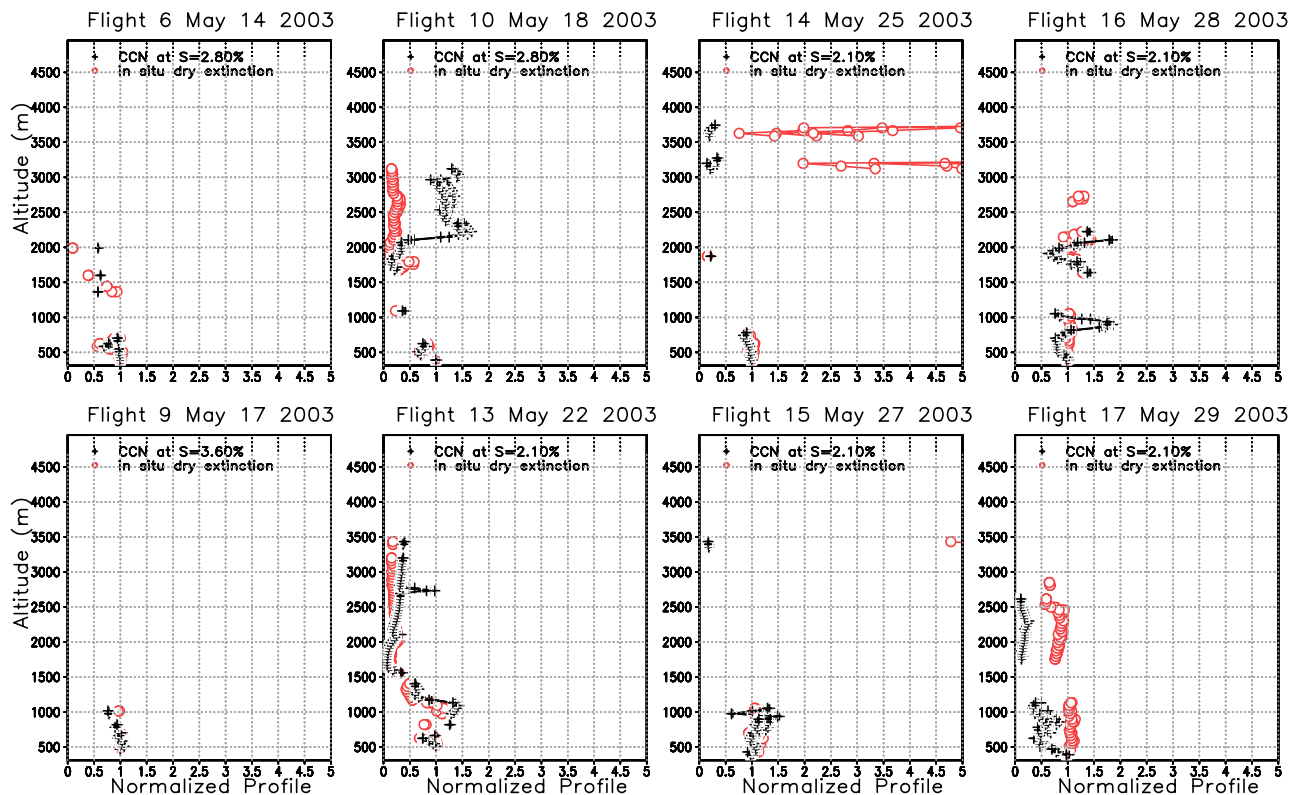


**Figure 1.** Vertical distribution of in situ measurements of the mean, mean plus standard error, and mean minus standard error of dry extinction (467 nm) and CCN concentration measured over the ARM site from the aircraft, at the supersaturation  $S$  indicated, on each of eight flights. Values have been normalized by the value at the lowest level with valid data for both profiles.

an evaluation tells us much more about the conditions that degrade the performance.

[30] Although normalization removes the absolute concentration from the evaluation and hence prevents examination of the skill in retrieving CCN variability from day to day, if much of that variability is captured by surface CCN measurements then there is little additional information for the retrieval to provide. Normalization focuses the evaluation on the additional information provided by the retrieval. We assume that surface CCN measurements provide reliable measurements of the variability of CCN concentrations near the surface.

[31] The retrievals of dry extinction and backscatter from surface instruments are subject to both retrieval error and sampling error. Before testing the validity of equation (1) using the retrieved dry extinction and backscatter, it is worth first testing using the in situ measurements of dry extinction. Figure 1 compares the vertical profile of the normalized in situ measurements of dry extinction (at 467 nm wavelength) with normalized in situ measurements of CCN for eight flights. The CCN concentration has considerable vertical structure, with concentrations varying by a factor of at least two and in most cases five. The vertical profile of normalized dry extinction closely follows that of CCN concentration on most flights, particularly within the lowest km above the surface. This agreement is surprising, considering the high supersaturation and hence (assuming the particles are hygroscopic) small characteristic size of the CCN measurements. Consistent with this finding, *Rissman et al.* [2006]

show that most CCN on these flights are highly insoluble and hence have lower hygroscopicity and larger sizes than highly soluble particles would have at that supersaturation. The larger size is consistent with the particles influencing extinction as well as CCN concentration.

[32] On some flights the vertical profile of normalized dry extinction does not follow that of CCN concentration. On flight 10 the normalized dry extinction significantly underestimates the normalized CCN concentration at altitudes between 2 and 3 km, suggesting a higher proportion of small particles (diameters less than 0.1 micron) there than near the surface; independent measurements of the particle size distribution confirm this. On flights 14 and 15 the normalized dry extinction increases dramatically above 3 km, while the normalized CCN concentration does not. This is due to the presence of an elevated plume of aged particles, most likely from forest fires in Siberia [*Damoah et al.*, 2004; *Jaffe et al.*, 2004]. DMA measurements show a large increase in the concentration of accumulation mode particles in the layer, which increases the extinction but not the CCN concentration. On flight 17, the normalized dry extinction overestimates the normalized CCN concentration at almost all levels, suggesting a greater presence of small particles near the surface.

[33] Table 2 lists 95% confidence limits of the square of the correlation between CCN concentration and in situ dry extinction for each flight. The confidence limits were determined using Fisher's  $Z$  transformation with the number of samples assumed to be the number of matching points in

**Table 2.** Ninety-Five Percent Confidence Intervals of Square of Correlation Between  $x$  and  $y$  for Eight Flights<sup>a</sup>

$x$	$y$	Flight							
		6	9	10	13	14	15	16	17
CCN1	in situ ext	0.13–0.87	0.08–0.93	–0.19–0.02	0.75–0.90	–0.62 to –0.02	–0.92 to –0.57	0.12–0.64	0.41–0.78
CCN1	RL ext	–0.84 to –0.01	–0.38–0.60	–0.37 to –0.01	0.19–0.56	–0.90 to –0.52	–0.26–0.12	–0.01–0.32	0.59–0.86
CCN1	RL bscat	–0.70–0.07	–0.01–0.86	–0.37 to –0.01	0.39–0.71	–0.90 to –0.52	–0.23–0.14	0.00–0.38	0.59–0.86
CCN1	MPL ext	...	...	–0.88 to –0.06	0.82–0.99	–0.99–0.00	0.00–0.96	–0.26–0.60	–0.48–0.52
CCN1	MPL bscat	...	...	–0.87 to –0.04	0.17–0.93	–0.99 to –0.17	–0.10–0.92	–0.25–0.61	–0.69–0.26
in situ ext	RL ext	–0.86 to –0.02	–0.66–0.30	0.36–0.74	0.25–0.62	0.12–0.74	–0.20–0.17	0.07–0.56	0.56–0.84
in situ ext	MPL ext	...	...	–0.17–0.61	0.92–0.99	0.02–0.99	–0.03–0.94	–0.54–0.34	–0.41–0.58
CCN	in situ ext	–0.17–0.90	0.04–0.97	0.00–0.59	0.92–0.99	–0.79–0.00	–0.76–0.54	–0.40–0.09	0.38–0.87
@ S = 0.1%									
CCN	in situ ext	–0.41–0.82	0.08–0.97	–0.51–0.00	0.63–0.93	–0.84 to –0.03	–0.67–0.65	–0.06–0.43	0.46–0.90
@ S = 1%									
CCN	CCN1	–0.31–0.86	0.02–0.94	0.00–0.57	0.77–0.96	0.89–0.99	–0.82–0.40	–0.21–0.36	0.60–0.93
@ S = 0.1%									
CCN	CCN1	–0.52–0.76	0.14–0.96	0.31–0.84	0.77–0.96	0.92–0.99	–0.78–0.49	0.00–0.71	0.28–0.84
@ S = 1%									

<sup>a</sup>Negative values denote negative correlations. Ext denotes extinction, and bscat denotes 180° backscatter.

Figure 1. In situ dry extinction explains 75–90% of the variance of CCN concentration on flight 13 and 41–78% of the variance on flight 17. The correlation might also be high on flights 6, 9, and 16, but the sample size is too small to permit a reliable estimate of the correlation. The high correlation on flight 15 is a negative correlation due to the elevated plume at 3400 m, the negative correlation indicating a failure of the retrieval scheme. The poor correlation on

two of the other three flights reflects deviations in the upper troposphere; dry extinction is highly correlated with CCN concentration in the lowest 1–2 km on those flights.

[34] The Raman lidar (RL) is one potential aerosol remote sensing tool for scaling surface CCN measurements. It provides retrievals of both extinction and backscatter at 355 nm wavelength. Figure 2 compares vertical profiles of the dry extinction and backscatter, normalized by the value

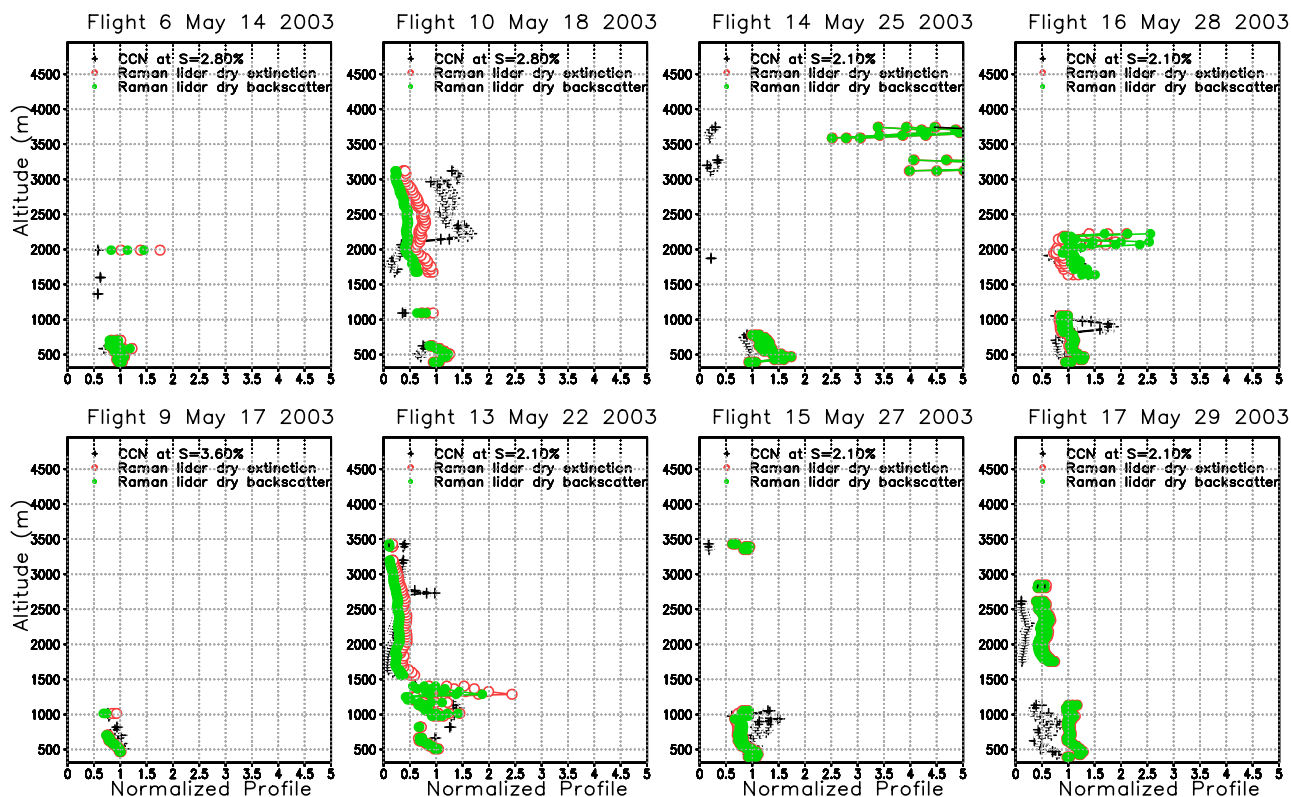


**Figure 2.** Vertical distribution of the mean, mean plus standard error, and mean minus standard error of CCN concentration measured over the ARM site from the aircraft and Raman lidar retrievals of extinction and backscatter, adjusted to dry conditions using the humidification factor measured on the aircraft, on each of eight flights. Values have been normalized by the value at the lowest level with valid data for all profiles.

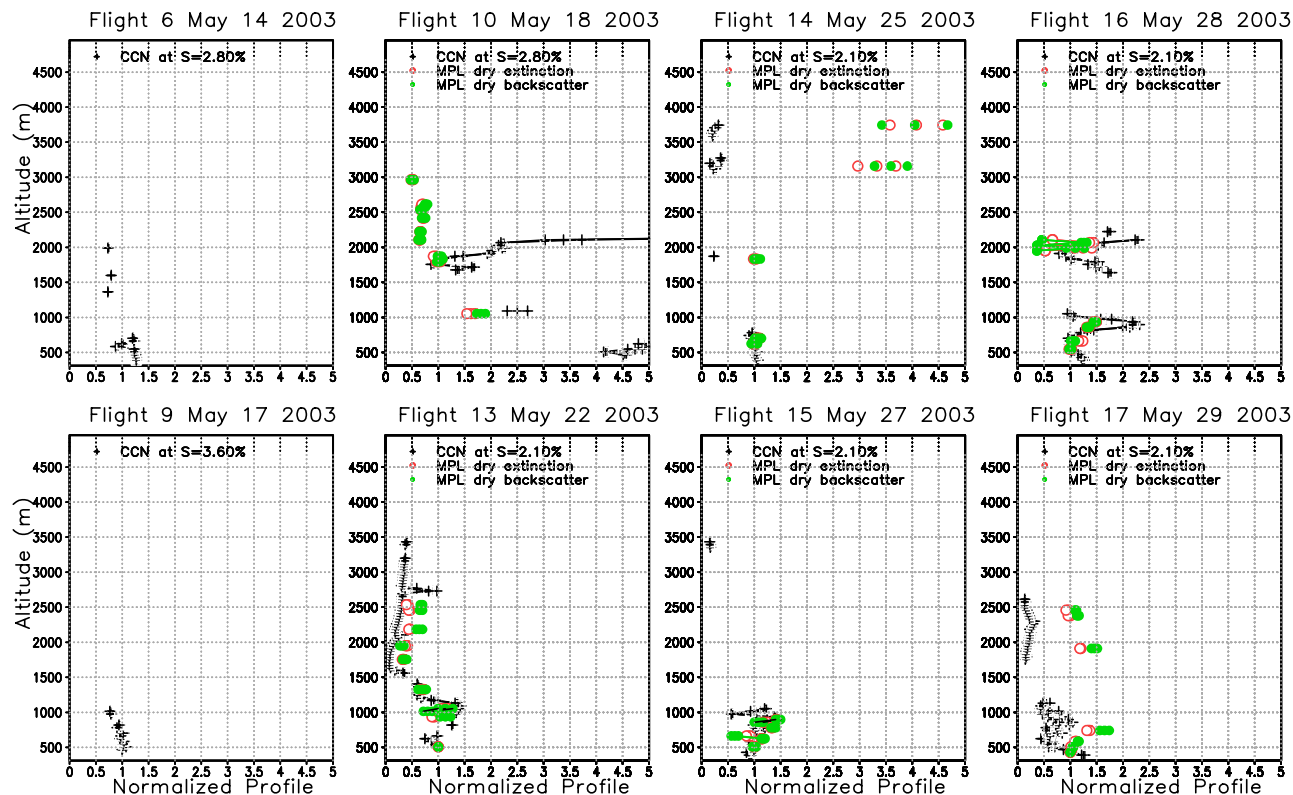


**Figure 3.** Vertical distribution of the mean, mean plus standard error, and mean minus standard error of CCN concentration measured over the ARM site from the aircraft and micropulse lidar retrievals of extinction and backscatter, adjusted to dry conditions using the humidification factor measured on the aircraft, on each of eight flights. Values have been normalized by the value at the lowest level with valid data for all profiles.

at the lowest level, with the vertical profile of the normalized CCN concentration. To separate errors due to remote sensing of relative humidity and the use of surface humidification measurements, the extinction and backscatter retrieved at ambient humidity have been adjusted to dry conditions using the humidification factor measured on aircraft instead of at the surface (retrievals adjusted using surface measurements of humidification and remote sensing of relative humidity will be considered later in this section).

[35] In general the Raman lidar retrievals of vertical profiles of normalized dry extinction and backscatter exhibit similar vertical structure and are comparably but somewhat more weakly correlated with CCN concentration compared with the in situ measurements of dry extinction. Many of the same profile differences evident for in situ measurements in Figure 1 are also evident for the Raman lidar retrievals shown in Figure 2. On flights 10 and 14 the same differences between normalized CCN concentration and normalized dry extinction above 2 km are evident for both the in situ and remote measurements of dry extinction, producing negative correlations between extinction and CCN concentration. The Raman lidar is clearly showing that dry extinction should not be used to scale CCN concentration for those conditions. On two other flights (13 and 17) the normalized dry extinction and backscatter follow the normalized CCN concentration rather well, with correlations (Table 2) comparable to those for in situ measurements of

dry extinction. On flights 10 and 16 the retrieved dry extinction and backscatter both correlate poorly with CCN concentration, as is the case for the in situ measurement of dry extinction. On flights 6, 9 and 15 the CCN concentration is correlated much less with the Raman lidar retrievals than the in situ extinction, but for all three flights there is very little vertical structure in CCN concentration.

[36] There is little difference between the normalized dry extinction and backscatter profiles on most days, suggesting that the extinction/backscatter ratio profile is nearly uniform on those days.

[37] The micropulse lidar (MPL) is another potential aerosol remote sensing tool for scaling surface CCN measurements. It provides retrievals of both extinction and backscatter at 523 nm wavelength, but assumes a constant extinction/backscatter ratio. Figure 3 compares vertical profiles of the dry extinction and backscatter, normalized by the value at the lowest level, with the vertical profile of the normalized CCN concentration. The extinction and backscatter retrieved at ambient humidity have been adjusted to dry conditions using the humidification factor measured on aircraft instead of at the surface.

[38] The normalized dry extinction and backscatter retrieved by the MPL do not appear to explain much of the variance of normalized CCN concentration on all flights except flight 13. The square of the correlation (Table 2) is at least 80% for flight 13, but the sample size is so low for the

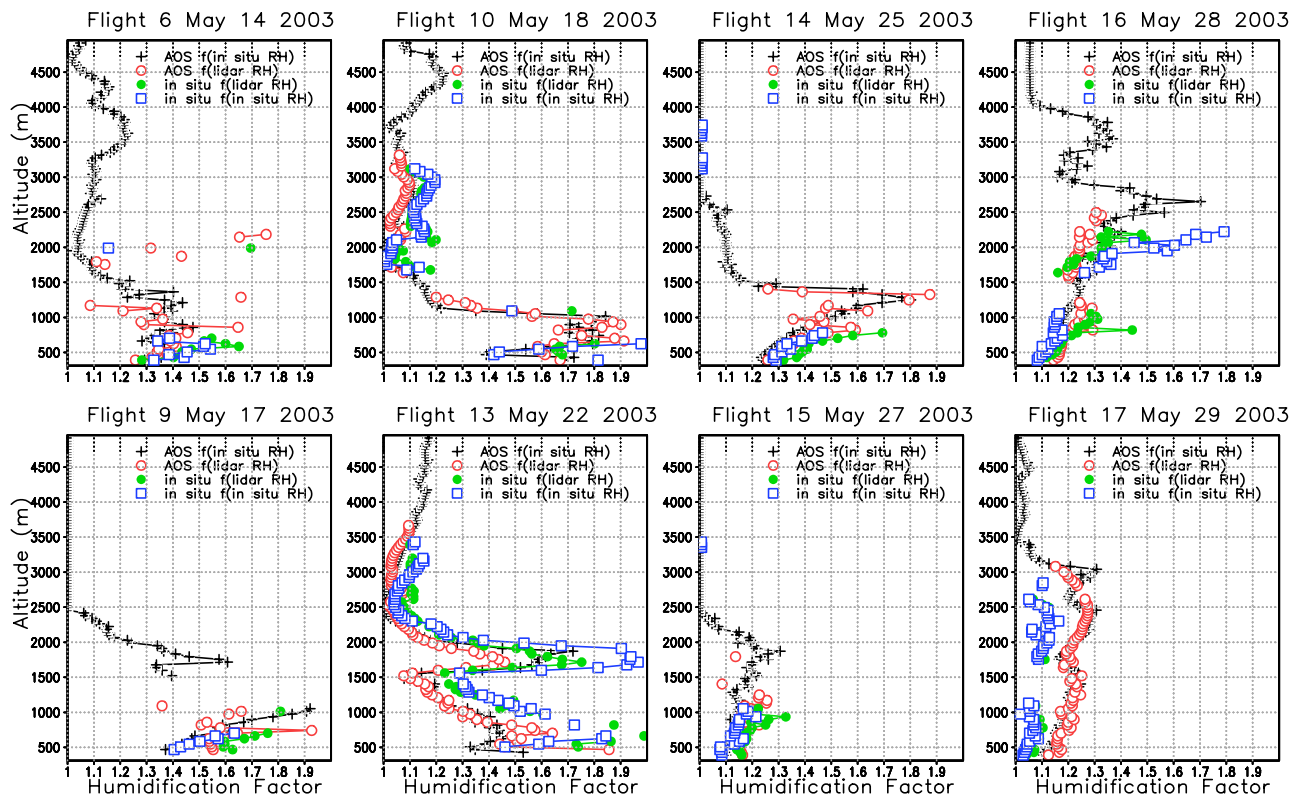


**Figure 4.** Vertical profiles of the humidification factor determined from the parameters of the humidification factor measured either from aircraft (in situ) or from the surface (AOS) and using relative humidity measured either from aircraft or from the Raman lidar retrieval of water vapor.

other flights that the uncertainty in the correlation is too large to draw conclusions. On most days there is little difference between the normalized extinction and backscatter because the MPL retrieval uses a single value for the extinction/backscatter ratio for each retrieval, but there are differences on some days because different retrievals (and different extinction/backscatter ratios) are used for different altitudes because the aircraft sampled the altitudes over the site at different times during its typical 4-hour flight.

[39] Given the high correlation between CCN concentration and in situ dry extinction, it is not surprising that the correlation between CCN concentration and remote sensing estimates of dry extinction is related to how well the remote sensing estimates correlate with the in situ measurement (Table 2). The correlations between CCN concentration and remote sensing estimates of dry extinction are only high if the correlations between CCN concentration and in situ dry extinction are high and the correlation between in situ dry extinction and estimates from remote sensing are also high. The former is true if the aerosol size distribution and composition are uniform or if the supersaturation is below 0.1% (GC), and latter is true only if the remote sensing estimates are not degraded by retrieval limitations or sampling errors. Both conditions must be satisfied before the remote sensing estimates are highly correlated with CCN concentration.

[40] How important is humidification in the retrieval, and how great is the uncertainty in its retrieval? Figure 4 shows vertical profiles of the humidification factor determined four

ways, using the parameters of the humidification factor measured either from aircraft or from the surface, and using relative humidity measured either from aircraft or from the Raman lidar retrieval of water vapor. The humidification factor varies widely, as much as a factor of two, in the vertical on some days. Clearly this vertical structure must be accounted for in the retrieval. On most days all four vertical profiles agree remarkably well, to within 20%, suggesting that retrieval of the vertical distribution of the humidification factor will not be a significant error source in the retrieval. The consistency of the humidification factor determined using in situ and remote sensing of relative humidity suggest that the retrieval of relative humidity is not a significant source of uncertainty, except as demonstrated on flight 13 when relative humidity approaches 100% and the humidification factor becomes large. The difference on flight 17 is clearly due to different values of the humidification exponent  $\gamma$ . The difference is evident even near the surface. It is not clear why the exponent is different on flight 17 but not on other flights.

[41] As stated previously, we would expect the CCN retrieval scheme to perform better at lower supersaturations. Although in situ CCN measurements on the Twin Otter are not available at supersaturations less than 2%, CCN concentrations at lower supersaturations can be estimated from Köhler theory using the measured size distribution and an assumed composition. We assume all particles are composed of ammonium sulfate. Although *Rissman et al.* [2006] conclude that a significant fraction of particles with

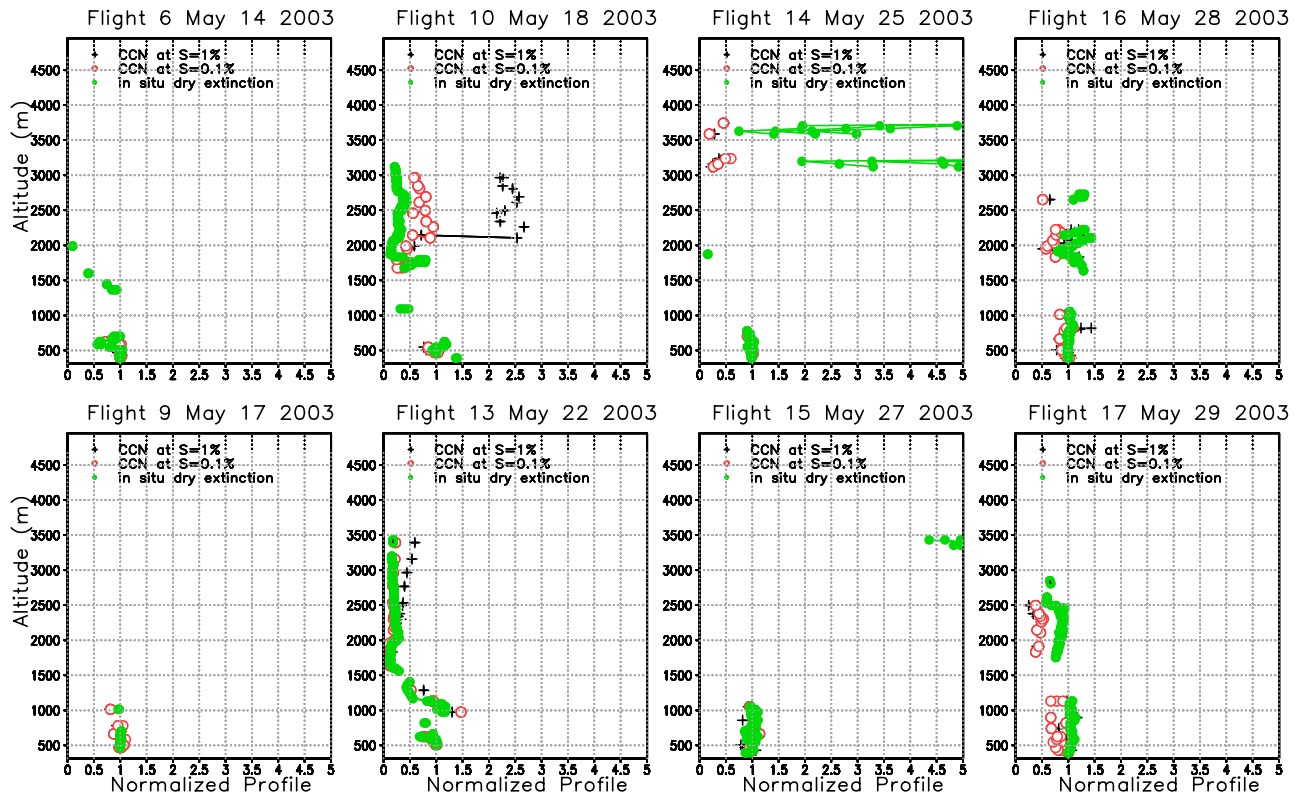


**Figure 5.** Vertical distribution of the mean, mean plus standard error, and mean minus standard error of in situ measurements of dry extinction and CCN concentration calculated from Köhler theory using aircraft measurements of aerosol size distribution at supersaturations of 0.1% and 1% on each of eight flights. Values have been normalized by the value at the lowest level with valid data.

diameter  $<50$  nm are dominated by insoluble material, we assume pure ammonium sulfate here simply to illustrate the dependence of the retrieval performance on particle size. Extinction depends much less on composition than on particle size at low relative humidity. We could easily choose a smaller hygroscopicity for the particles and a smaller critical supersaturation to focus on the same size range of particles. Figure 5 shows vertical profiles of the in situ measurement of dry extinction and the CCN concentration estimated at 0.1% and 1% supersaturation, all normalized by their values at the lowest available level. The vertical profile of the normalized CCN concentration estimated at 1% supersaturation is very similar to the CCN measurements shown in Figure 1. Indeed, as listed in Table 2 the squared correlation between the CCN measurement and that estimated at 1% is at least 0.6 on all but three flights. As expected, the agreement between the dry extinction and estimated CCN concentration is clearly better for the CCN concentration at 0.1% than at 1%, particularly above the boundary layer for flights 10 and 13. This visual interpretation is confirmed by the higher squared correlation with dry extinction for CCN concentration estimated at 0.1% than at 1%, as listed in Table 2, for those flights. The better agreement at 0.1% is encouraging, because such a supersaturation is considered to be more typical of boundary layer clouds under continental conditions [Hudson and Yum, 2001, 2002; Yum and Hudson, 2002]. On flight 14 dry extinction above 3 km does not correlate well with the estimated CCN concentration at either supersaturation,

which suggests that the elevated plume there has a different size distribution or composition than in the boundary layer. For almost all flights correlations are higher if the soluble fraction of the particles is assumed to be 0.2 rather than 1.0, which shifts the mean size of CCN closer to the accumulation mode size of the particles that dominate extinction.

[42] Could sampling errors due to spatial/temporal variability explain the weaker relationship between CCN concentration and remote retrievals of dry extinction and backscatter than between CCN concentration and in situ measurements of dry extinction? We have found the relationship to be insensitive to the spatial and temporal range of the sampling filter for distances between 5 and 30 km and time differences between 15 and 60 min. Figure 6 provides further evidence that sampling errors for RH profiles are small. The relative humidity retrieved from Raman lidar measurements agrees remarkably well with in situ measurements. This suggests that spatial/temporal sampling error does not contribute much to the differences between the CCN profiles and the retrieved profiles of extinction and backscatter.

[43] We have noted that the presence of elevated layers of aerosol with very different size distributions or compositions can degrade the performance of the retrieval scheme. Della Monache *et al.* [2004] conclude that aerosol properties above the mixed layer are poorly correlated with those within the boundary layer. To further test this hypothesis, we have recalculated the correlations of Table 2 for only levels within the mixed layer. We use Heffter's [1980]

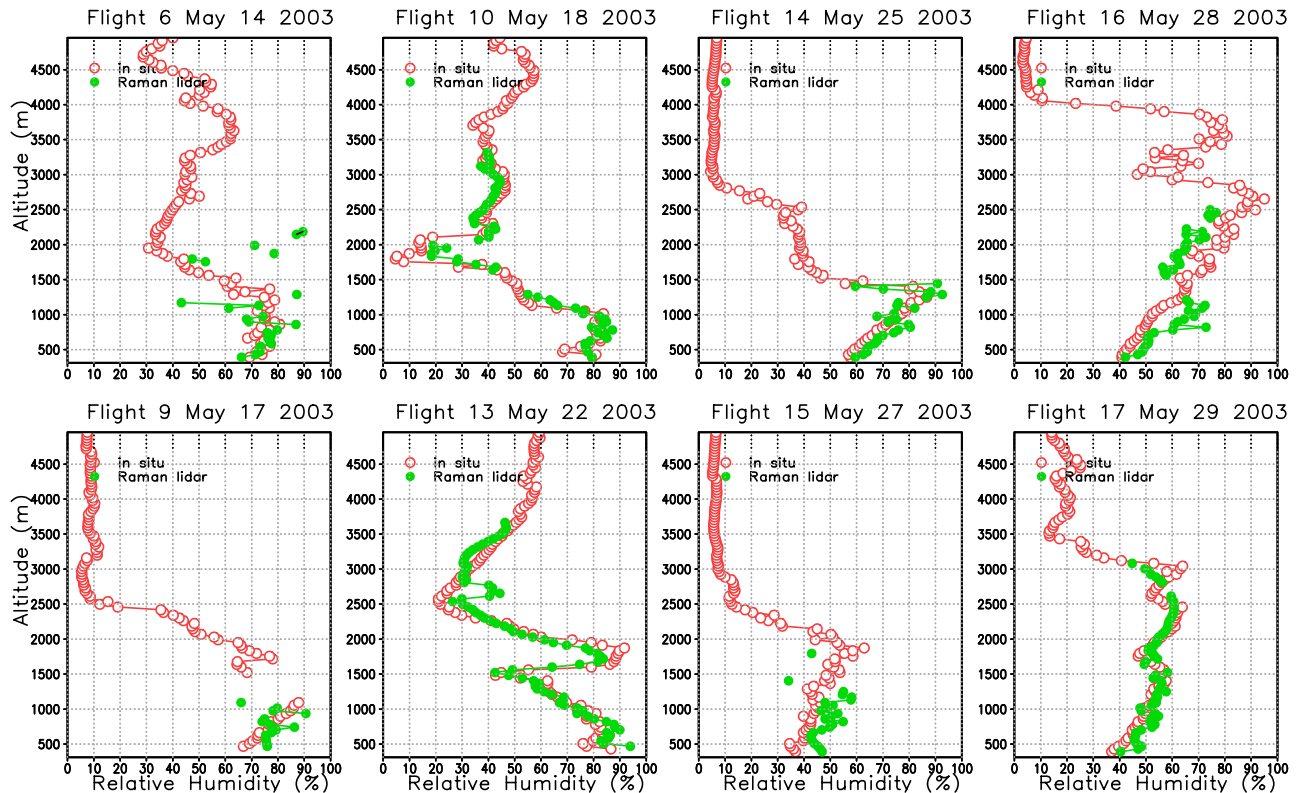


**Figure 6.** Vertical profile of relative humidity retrieved by Raman lidar and measured by aircraft for eight flights. Raman lidar retrievals are only if estimated error  $<25\%$ .

definition of the mixed layer height, which is the lowest level in the inversion layer where the difference between the potential temperature at that level and at the base of the inversion layer exceeds  $2^{\circ}\text{C}$ , where the inversion layer is defined by the condition that potential temperature increases with altitude at a rate exceeding  $0.005^{\circ}\text{C m}^{-1}$ . Table 3 lists the same correlations as those in Table 2, except that it is only over levels within the mixed layer. As expected, the large negative correlations associated with elevated plumes have been eliminated, particularly on flights 14 and 15. However, the positive correlations on other flights, such as 13 and 17, have been reduced because variance above the mixed layer that had been explained in Table 2 has now been filtered out. By limiting the retrieval to the mixed layer, which is highly correlated with the surface [della Monache *et al.*, 2004], little improvement over surface

values is permitted. If cloud base is above the mixed layer much more can be gained by extending the retrieval above the mixed layer, provided the accuracy of the retrieval there can be estimated independently. Doing so will not affect the retrieval for the boundary layer. Estimating the accuracy is addressed in section 3.3.

### 3.2. Evaluation of Full Retrieval

[44] As a final test combining all sources of uncertainty, Figure 7 compares vertical profiles of retrieved and estimated (from DMA size distribution) CCN concentrations at 0.1% and 2% supersaturation and measured CCN concentration at the indicated supersaturation. The retrieval scales the surface measurement of CCN concentration by the Raman lidar retrieval of ambient extinction divided by the humidification factor at the retrieved relative humidity using

**Table 3.** As in Table 2, but Only for Points Within the Mixed Layer

x	y	Flight							
		6	9	10	13	14	15	16	17
CCN1	in situ ext	0.47–0.97	0.08–0.93	0.65–0.99	0.00–0.83	0.00–0.80	–0.36–0.09	0.00–0.51	–0.31–0.11
CCN1	RL ext	–0.45–0.43	–0.38–0.60	–0.90–0.16	–0.05–0.77	–0.12–0.60	–0.46–0.03	–0.56–0.00	–0.07–0.36
CCN1	RL bscat	–0.36–0.52	–0.01–0.86	–0.89–0.22	–0.11–0.72	–0.11–0.60	–0.54–0.01	–0.34–0.06	–0.08–0.35
CCN1	MPL ext	...	...	...	...	...	0.00–0.96	–0.21–0.99	–0.92–0.45
CCN1	MPL bscat	...	...	...	...	...	–0.10–0.92	0.22–0.99	–0.92–0.47
in situ ext	RL ext	–0.25–0.61	–0.66–0.30	–0.94–0.02	0.00–0.84	–0.09–0.63	–0.37–0.09	–0.34–0.06	–0.33–0.10
in situ ext	MPL ext	...	...	...	...	...	–0.03–0.94	–0.71–0.98	–0.76–0.79
CCN @ S = 0.1%	in situ ext	–0.17–0.90	0.04–0.97	–0.65–0.99	–0.44–0.99	–0.12–0.92	–0.76–0.54	–0.56–0.43	–0.83–0.00
CCN @ S = 1%	in situ ext	–0.41–0.82	0.08–0.98	–0.73–0.98	–0.28–0.99	–0.50–0.78	–0.67–0.65	–0.15–0.76	–0.12–0.71
CCN @ S = 0.1%	CCN1	–0.31–0.86	0.02–0.94	–0.69–0.98	0.04–0.99	–0.03–0.94	–0.82–0.40	0.48–0.98	–0.01–0.82
CCN @ S = 1%	CCN1	–0.52–0.76	0.14–0.96	–0.75–0.98	0.45–0.99	–0.40–0.82	–0.78–0.49	0.47–0.98	–0.32–0.55

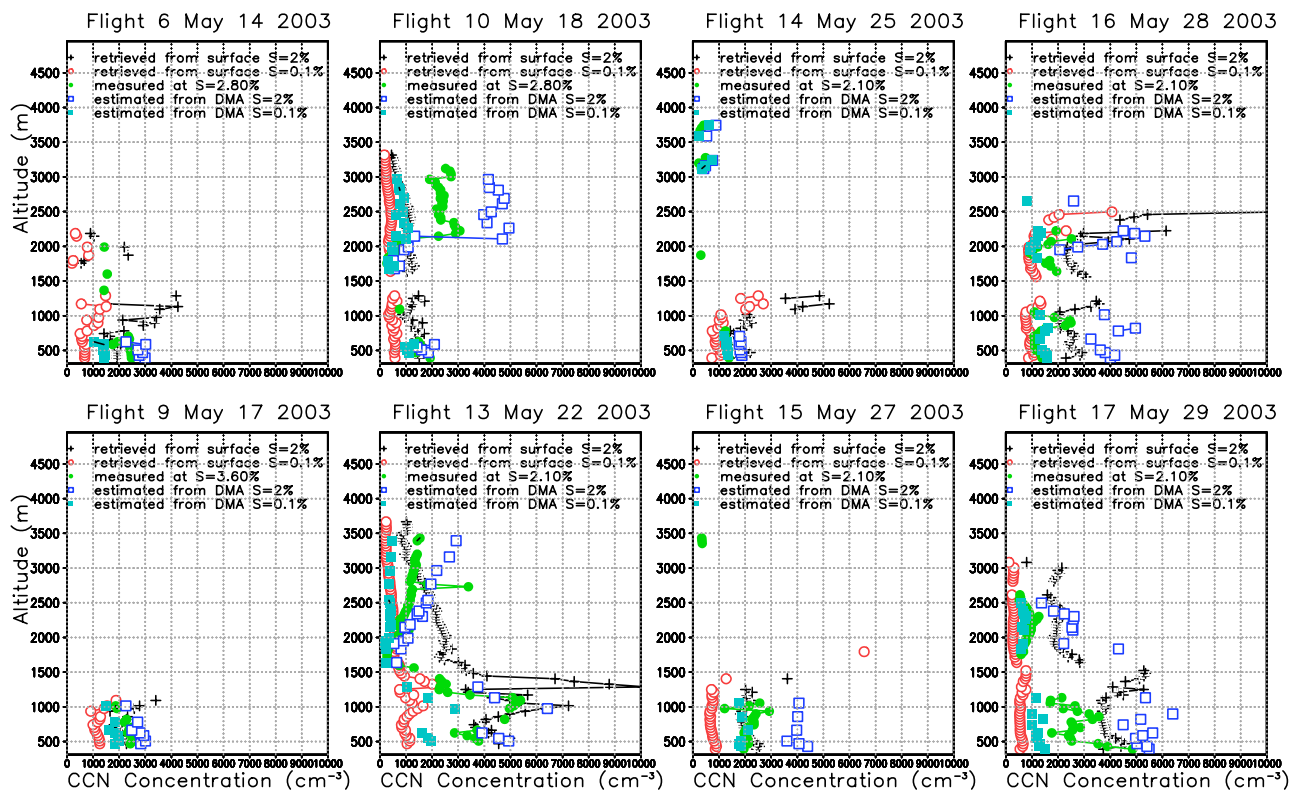


**Figure 7.** Vertical profiles of retrieved and estimated (from DMA size distribution) CCN concentrations at 0.1% and 1% supersaturation and measured CCN concentration at the indicated supersaturation for each flight. The retrieval scales the surface measurement of CCN concentration by the Raman lidar retrieval of ambient extinction divided by the humidification factor at the retrieved relative humidity using the surface measurement of the humidification function.

the surface measurement of the humidification function. The same scaling profile is therefore applied to the surface CCN measurements at both supersaturations. This is an especially difficult test because even if the retrieval were perfect it would still differ from the in situ measurements because of differences between the surface CCN instrument, the aircraft CCN instrument, and the estimate using the measured size distribution and an assumed ammonium sulfate composition.

[45] Yet some skill (relative to surface values) is evident in the retrieval when the vertical structure in the CCN profile is not dominated by variations in aerosol composition or in the aerosol size distribution. On the flight with the best performance of the CCN retrieval scheme (13), the retrieval of CCN at  $S = 2\%$  captures the increase with altitude up to 1000 m and then the decrease with altitude up to 1600 m. Although the agreement is not as good as the agreement between the in situ CCN measurement and CCN estimated from the measured size distribution, useful skill is clearly evident. At  $S = 0.1\%$  the agreement is also quite good, not only up to 1600 but up to at least 3500 m. On other days the performance is marginal with skill generally limited to the boundary layer. As we have already seen, the performance above the boundary layer is on some flights (14, 15, and 16) limited by the presence of an aerosol layer aloft with very different microphysical characteristics. Identifying such conditions is therefore important for determining when CCN concentrations can

be retrieved with confidence. This question is addressed in the next section.

### 3.3. Estimating Retrievalability From the Surface

[46] Given the variable performance of the CCN retrieval scheme, its value would be greatly enhanced if there was some independent way to estimate its accuracy. GC suggested that Raman lidar retrievals of the extinction to backscatter ratio, which depends on particle size, could be used to distinguish conditions in which the particle size distribution and composition are uniform (when one would expect the CCN retrieval scheme to work best) or stratified (when the CCN retrieval scheme should perform poorly unless the CCN concentration is dominated by the same particles that control extinction). We have looked at the vertical structure of the extinction to backscatter ratio for the flights during this experiment, and conclude that the degraded sensitivity of the Raman lidar during the experiment limited the accuracy and hence the utility of the ratio as an indicator of vertical structure in the aerosol size distribution and composition.

[47] To assess the potential value of extinction/backscatter retrievals from a healthy Raman lidar, we can look at vertical profiles of the dry hemispheric backscatter fraction and of the Ångström exponent determined from in situ measurements. The hemispheric backscatter fraction  $b$  is defined as the ratio of the dry hemispheric backscattering to the dry total scattering. Larger values of  $b$  indicate particles

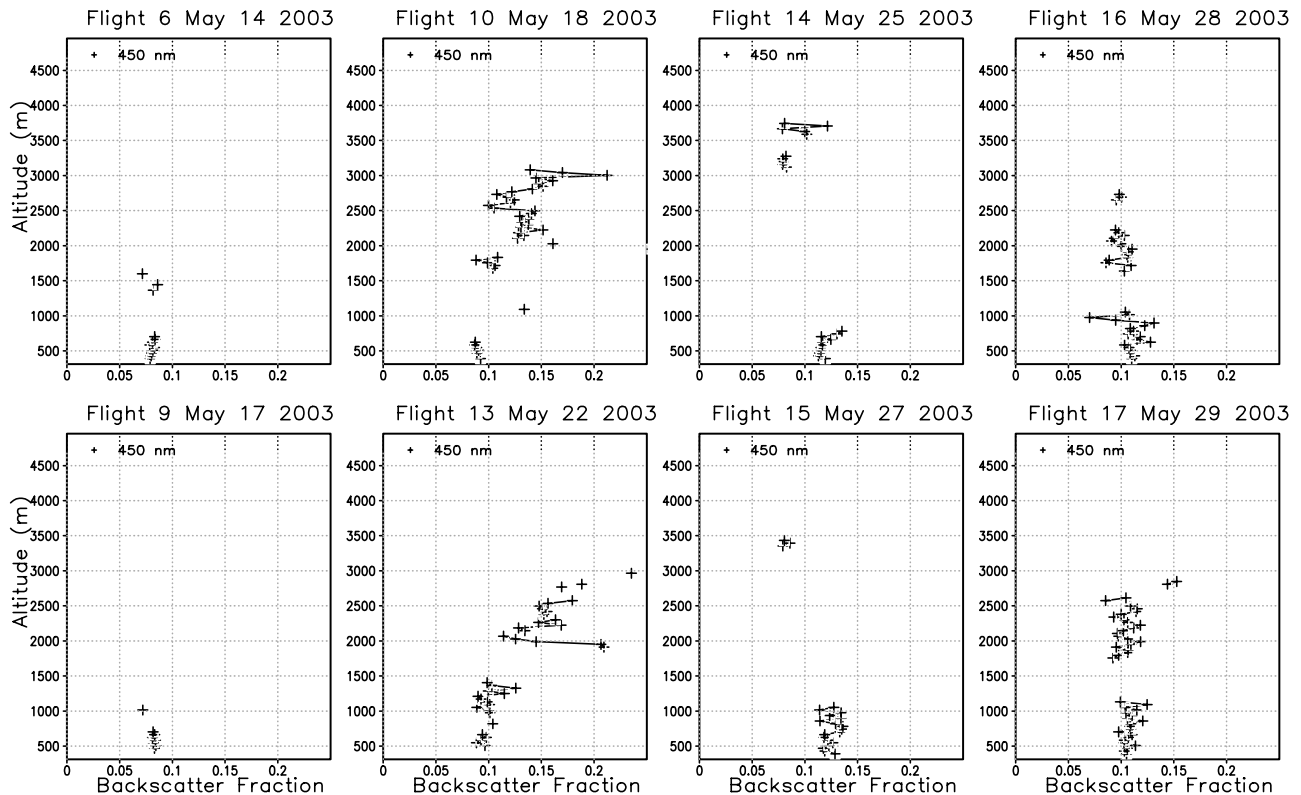


**Figure 8.** Vertical profile of dry hemispheric backscatter fraction at 450 nm for eight flights.

in the optical range 100–500 nm are shifted toward the smaller end of the range. The Ångström exponent, which is the exponent in a power law approximation for the wavelength-dependence of scattering,  $\sigma_s \sim \lambda^{-\hat{a}}$ , is determined from the dry scattering measured at two different wavelengths:  $\hat{a}(\lambda_1, \lambda_2) = \ln(\sigma_2/\sigma_1)/\ln(\lambda_1/\lambda_2)$  where  $\sigma_1$  and  $\sigma_2$  are the dry scattering at wavelengths  $\lambda_1$  and  $\lambda_2$ . The Ångström exponent is near zero in the geometric optics limit of particles much larger than the wavelength, and near four in the Rayleigh limit of particles much smaller than the wavelength. Hence larger values of  $\hat{a}$  indicate a larger proportion of scattering contributed by particles smaller than the wavelength, i.e., with radius less than 80 nm.

[48] Figure 8 shows vertical profiles of the hemispheric backscatter fraction at 450 nm. One might expect the backscatter fraction to be most uniform on flight 13, which is when the CCN retrieval scheme performs best. Contrary to this expectation, the vertical profile of backscatter fraction is least uniform on flight 13, increasing more than twofold between the surface and 3000 m. On flights that we might expect vertical structure in the backscatter fraction, we find that the vertical structure is consistent with expectations. On flight 10, which according to the DMA measurements has an elevated plume of ultrafine particles (diameter less than 100 nm) that produce higher CCN concentrations at altitudes between 2000 and 3000 m, the backscatter fraction increases with altitude, which also indicates a shift toward smaller particles within the optical size range. In the elevated plume on flights 14 and 15, which according to the DMA measurements has reduced ultrafine particle concentrations and higher accumulation mode particles (diameters between 100 and 500 nm), the backscatter fraction is lower

than in the mixed layer, which as expected implies a shift toward larger particles within the optical size range.

[49] Somewhat different conclusions follow from the vertical profile of Ångström exponent, shown in Figure 9. The exponent is lower in the elevated plume than in the mixed layer for flights 14 and 15, which suggests larger particles and hence is consistent with the DMA measurements and the bias in the retrieval. However, on flight 10 the exponent is lower in the plume than in the mixed layer (at least for 550–700 nm), which also suggests larger particles but is inconsistent with the higher concentration of ultrafine particles measured in the plume by the DMA. On flight 13 the moderate decrease in exponent with height is inconsistent with the increase in backscatter fraction and with the strong performance of the CCN retrieval scheme for that flight.

[50] These inconsistencies suggest that any reliability metrics based on measurements at visible wavelengths are of questionable value in predicting the performance of the retrieval scheme for the high supersaturations for which we have CCN measurements. At such high supersaturations the CCN concentration is often controlled by particles that are simply too small to influence optical measurements. At lower supersaturations the CCN concentration is more sensitive to the same particles that influence the aerosol optical properties, and hence we can expect higher performance of both the retrieval and optical metrics that might assess reliability. A reliability metric based on the Raman lidar, which operates at 355 nm, might be more useful than metrics based on visible wavelengths, but the degraded sensitivity of the Raman lidar prevented a direct evaluation of its potential for providing a useful reliability.

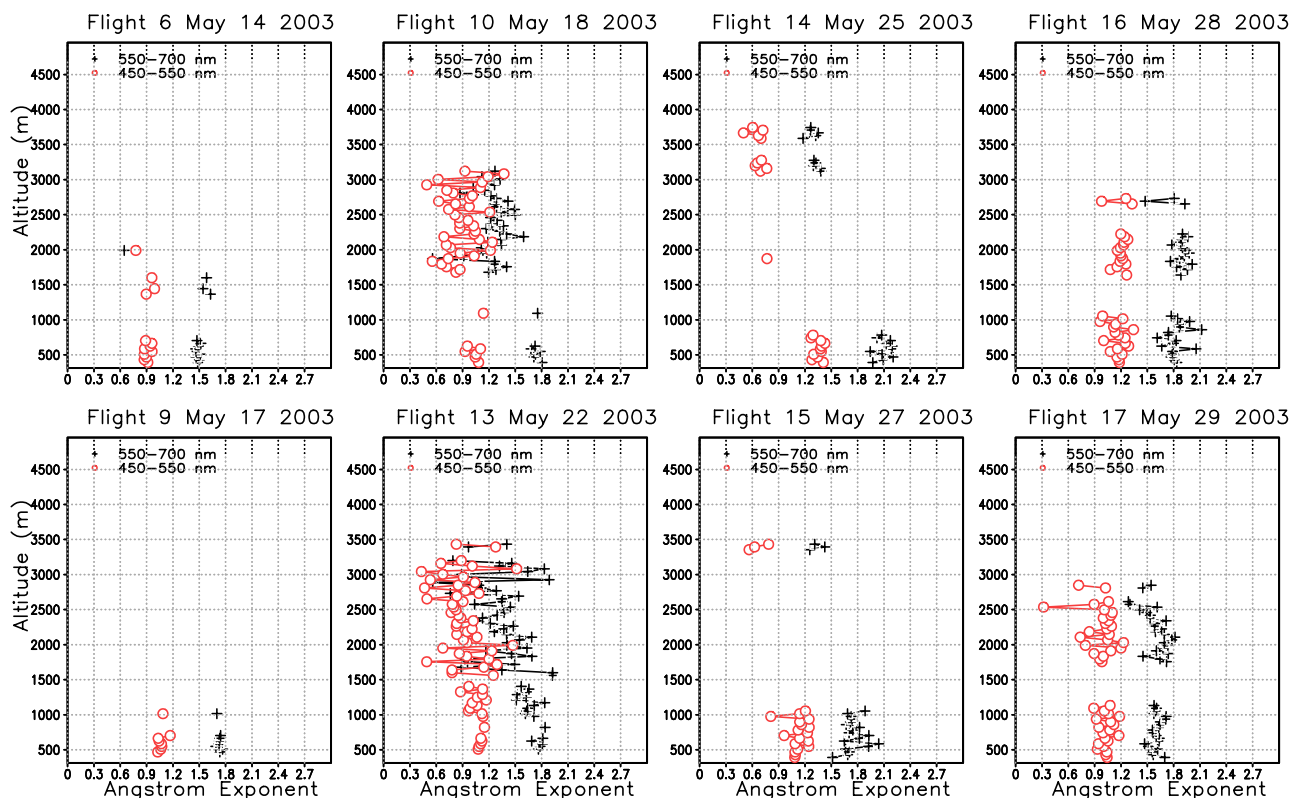


**Figure 9.** Vertical profile of Ångström exponent between 450 and 550 nm and between 550 and 700 nm for eight flights.

[51] Finally, one final metric from this IOP deserves some attention. The single-scattering albedo (the ratio of absorption to extinction) is controlled by the size distribution and chemical composition of the aerosol, and thus changes in the single-scattering albedo with altitude indicate conditions where the assumptions of the retrieval algorithm may not be valid. Although remote sensing of the vertical profile of single-scattering albedo is not currently feasible and hence we cannot expect single-scattering albedo to be a useful surface-based predictor of the performance of the CCN retrieval, we examine the vertical structure of the single-scattering albedo for evidence of vertical structure in aerosol composition as an explanation for biases in the CCN retrieval. Figure 10 shows vertical profiles of the single-scattering albedo (1- single-scattering albedo) for each flight. Higher albedo indicates more absorption. The largest variance is for flights 10 and 13, with somewhat higher albedo at higher altitudes. On flights 14 and 15 there is little difference between the albedo of the plume and mixed layers. It would appear that the particles controlling single-scattering albedo are not well correlated with the particles controlling the CCN number concentration, as the vertical profile of single-scattering albedo does not appear to explain much of the differences in performance of the CCN retrieval scheme on the flights studied here.

#### 4. Conclusions

[52] We have used a combination of aircraft, surface in situ, and surface remote sensing measurements to test various aspects of the GC scheme for retrieving CCN

concentration. Our analysis leads us to the following conclusions.

[53] 1. If in situ measurements of extinction are used, the performance of the CCN retrieval for the high supersaturations ( $>2\%$ ) of the in situ CCN measurements can be quite high, with  $r^2$  exceeding at least 0.4 on two and perhaps five of the eight flights examined, but can be negligible on other flights. GC arrived at a similar conclusion for pure ammonium sulfate particles and for supersaturations exceeding 1%, explaining the poor performance on some flights because CCN concentration at high supersaturations is dominated by particles too small to influence extinction or backscatter. Independent evidence [Rissman *et al.*, 2006] suggests a high insoluble content and hence low hygroscopicity and high critical supersaturation for particles large enough to influence extinction and backscatter as well as CCN concentration. The significant skill on such a large fraction of the flights suggests that degradation of the retrieval performance by stratification of the size distribution and composition is uncommon. It is worth noting that the poor performance on two of the flights was caused by a highly unusual elevated plume of large particles.

[54] 2. On some flights, correlations are significantly higher for supersaturations of 0.1% than for 1% because CCN concentrations at 0.1% are more likely to be controlled by the same particles that control extinction and backscatter. This conclusion is compromised by the absence of CCN measurements at these supersaturations and the need to assume a uniform composition when using Köhler theory to estimate CCN concentration from the measured aerosol size distribution.

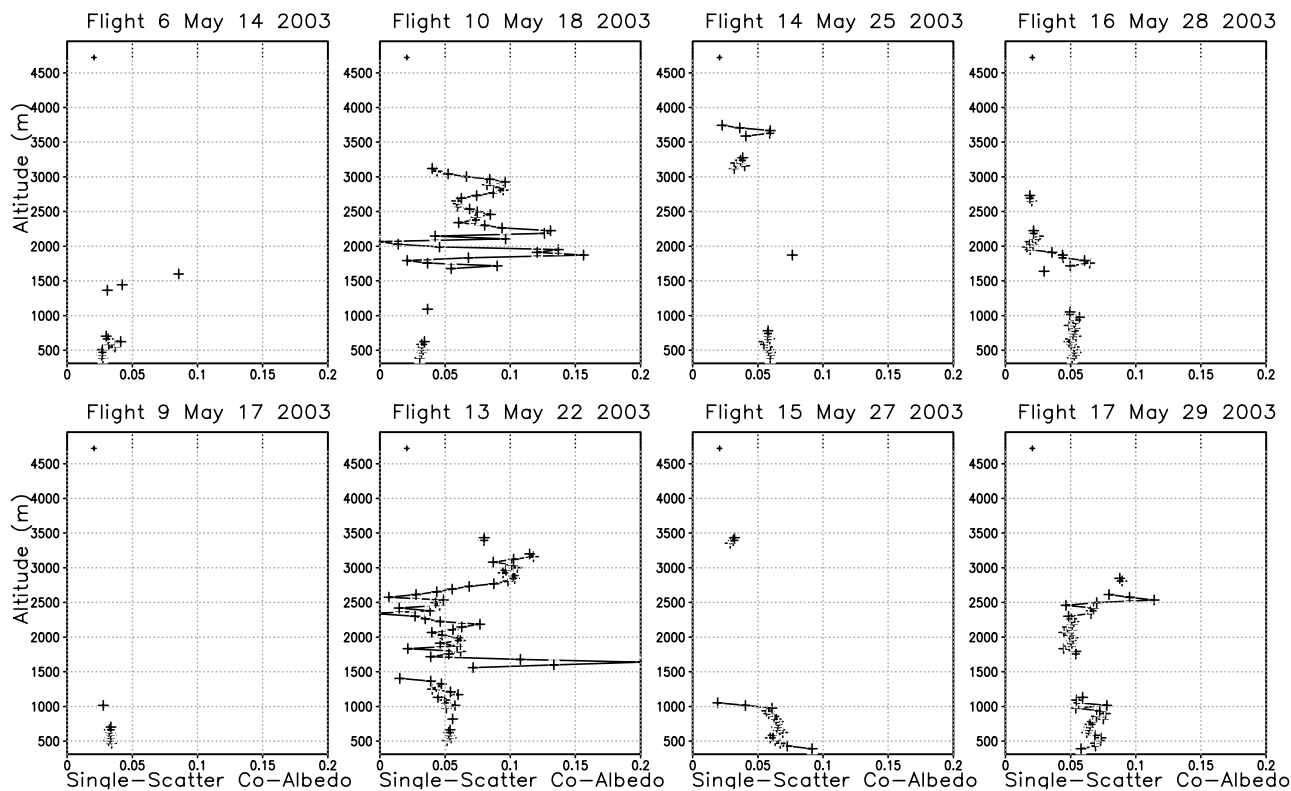


**Figure 10.** Vertical profile of single-scattering coalbedo for eight flights.

[55] 3. The retrieval of the vertical profile of the humidification factor is not the major limitation of the CCN retrieval scheme.

[56] 4. The performance of the retrieval varies significantly from day to day, particularly at supersaturations of 1% and higher, with higher correlations on days with uniform vertical profiles of size distribution.

[57] 5. Vertical inhomogeneity in the size distribution and presumably composition and particle shape are the dominant sources of error in the CCN retrieval.

[58] 6. Measurements of optical parameters that depend on the aerosol composition, shape and size distribution are not reliable predictors of the performance of the retrieval at high supersaturations because such measurements are based on visible wavelengths, which are insensitive to the particles that control CCN concentration at high supersaturations. A reliability metric based on the Raman lidar, which operates at 355 nm, might be more useful than metrics based on visible wavelengths, but the degraded sensitivity of the Raman lidar prevented a direct evaluation of its potential for providing a useful reliability.

[59] The evaluation of the retrieval scheme was compromised by three limitations. First, the Raman lidar was not performing up to its capability. This limited our interpretation of the full retrieval scheme. Second, the lack of in situ measurements of CCN concentration at supersaturations less than 2% limited our ability to evaluate the performance at low supersaturation. Estimating the CCN concentration at lower supersaturations using the measured size distribution and an assumed ammonium sulfate composition was clearly a significant compromise. Yet it served to illustrate important aspects of the retrieval performance. Third, the in situ CCN

measurements were not strictly collocated in time and space with the lidar retrievals. We did not find much sensitivity of the correlations to the collocation requirements, but this limitation still needs to be considered as a source of error.

[60] Further evaluation of the retrieval would therefore benefit from more reliable retrievals by ambient extinction and backscatter, and from in situ measurements of the full CCN spectrum. The sensitivity of the Raman lidar at the ARM CRF has been restored recently, and instruments to measure the full CCN spectrum are available and could be deployed in an experiment more focused on CCN.

[61] **Acknowledgments.** This study and the May 2003 Aerosol IOP were supported by the U.S. Department of Energy Atmospheric Radiation Measurement Program and Atmospheric Science Program, which are part of the DOE Biological and Environmental Research Program. The Pacific Northwest National Laboratory is operated for the DOE by Battelle Memorial Institute under contract DE-AC06-76RLO 1830.

## References

- Anderson, T. L., and J. A. Ogren (1998), Determining aerosol radiative properties using the TSI 3563 integrating nephelometer, *Aerosol Sci. Technol.*, *29*, 57–69.
- Anderson, T. L., S. J. Masonis, D. S. Covert, R. J. Charlson, and M. J. Rood (2000), In situ measurement of the aerosol extinction-to-backscatter ratio at a polluted, continental site, *J. Geophys. Res.*, *105*, 26,907–26,915.
- Brechtel, F. J., and S. M. Kreidenweis (2000a), Predicting particle critical supersaturation from hygroscopic growth measurements in the humidified TDMA. Part I: Theory and sensitivity studies, *J. Atmos. Sci.*, *57*, 1854–1871.
- Brechtel, F. J., and S. M. Kreidenweis (2000b), Predicting particle critical supersaturation from hygroscopic growth measurements in the humidified TDMA. Part II: Laboratory and ambient studies, *J. Atmos. Sci.*, *57*, 1872–1887.
- Conant, W. C., et al. (2004), Aerosol-cloud drop concentration closure in warm cumulus, *J. Geophys. Res.*, *109*, D13204, doi:10.1029/2003JD004324.

- Damoah, R., N. Spichtinger, C. Forster, P. James, I. Mattis, U. Wandinger, S. Beirle, T. Wagner, and A. Stohl (2004), Around the world in 17 days—Hemispheric-scale transport of forest fire smoke from Russia in May 2003, *Atmos. Chem. Phys. Discuss.*, *4*, 1449–1471.
- della Monache, L. D., K. D. Perry, R. T. Cederwall, and J. A. Ogren (2004), In situ aerosol profiles over the Southern Great Plains cloud and radiation test bed site: 2. Effects of mixing height on aerosol properties, *J. Geophys. Res.*, *109*, D06209, doi:10.1029/2003JD004024.
- Feingold, G., W. L. Eberhard, D. E. Veron, and M. Previdi (2003), First measurements of the Twomey indirect effect using ground-based remote sensors, *Geophys. Res. Lett.*, *30*(6), 1287, doi:10.1029/2002GL016633.
- Ferrare, R. A., D. D. Turner, L. H. Brasseur, W. F. Feltz, O. Dubovik, and T. P. Tooman (2001), Raman lidar measurements of the aerosol extinction-to-backscatter ratio over the Southern Great Plains, *J. Geophys. Res.*, *106*, 20,333–20,348.
- Ferrare, R., et al. (2004), Raman lidar measurements of aerosols and water vapor over the Southern Great Plains, *22nd International Laser Radar Conference*, edited by G. Pappalardo and A. Amodio, *Eur. Space Agency Spec. Publ., ESA SP-561*, 333–336.
- Ferrare, R., D. Turner, M. Clayton, V. Brackett, B. Schmid, J. Redemann, D. Covert, R. Elleman, J. Ogren, E. Andrews, J. Goldsmith, and H. Jonsson (2006), Evaluation of daytime measurements of aerosols and water vapor made by an operational Raman lidar over the Southern Great Plains, *J. Geophys. Res.*, doi:10.1029/2005JD005836, in press.
- Ghan, S. J., and D. R. Collins (2004), Use of in situ data to test a Raman lidar-based cloud condensation nuclei remote sensing method, *J. Atmos. Oceanic Technol.*, *21*, 387–394.
- Gultepe, I., G. A. Isaac, and W. R. Leitch (1998), Parameterizations of marine stratus microphysics based on in situ observations: Implications for GCMs, *J. Clim.*, *9*, 345–357.
- Hallberg, A., et al. (1997), Microphysics of clouds: Model vs measurements, *Atmos. Environ.*, *31*, 2453–2462.
- Han, Q., W. B. Rossow, J. Chou, and R. Welch (1998), Global variation in column droplet concentration in low-level clouds, *Geophys. Res. Lett.*, *25*, 1419–1422.
- Heffter, J. L. (1980), Transport layer depth calculations, paper presented at Second Joint Conference on Applications of Air Pollution Meteorology, Am. Meteorol. Soc., New Orleans, La., 24–28 March.
- Hudson, J. G. (1989), An instantaneous CCN spectrometer, *J. Atmos. Oceanic Technol.*, *6*, 1055–1065.
- Hudson, J. G., and S. S. Yum (2001), Maritime-continental drizzle contrasts in small cumuli, *J. Atmos. Sci.*, *58*, 915–926.
- Hudson, J. G., and S. S. Yum (2002), Cloud condensation nuclei spectra and polluted and clean clouds over the Indian Ocean, *J. Geophys. Res.*, *107*(D19), 8022, doi:10.1029/2001JD000829.
- Jaffe, D., I. Bertsch, L. Jaeglé, P. Novelli, J. S. Reid, H. Tanimoto, R. Vingarzan, and D. L. Westphal (2004), Long-range transport of Siberian biomass burning emissions and impact on surface ozone in western North America, *Geophys. Res. Lett.*, *31*, L16106, doi:10.1029/2004GL020093.
- Kim, B.-G., S. E. Schwartz, M. A. Miller, and Q. Min (2003), Effective radius of cloud droplets by ground-based remote sensing: Relationship to aerosol, *J. Geophys. Res.*, *108*(D23), 4740, doi:10.1029/2003JD003721.
- Lin, H., and R. Leitch (1997), Development of an in-cloud aerosol activation parameterization for climate modeling, paper presented at Workshop on Measurements of Cloud Properties for Forecasts of Weather, Air Quality, and Climate, World Meteorol. Organ., Geneva, Switzerland.
- Liu, Y., and P. H. Daum (2002), Indirect warming effect from dispersion forcing, *Nature*, *419*, 580–581.
- Menon, S., and V. K. Saxena (1998), Role of sulfates in regional cloud-climate interactions, *Atmos. Res.*, *47–48*, 299–315.
- Menon, S., V. K. Saxena, P. Durkee, B. N. Wenny, and K. Nielsen (2002), Role of sulfate aerosols in modifying the cloud albedo: A closure experiment, *Atmos. Res.*, *61*, 169–187.
- Menon, S., et al. (2003), Evaluating aerosol/cloud/radiation process parameterizations with single column models and ACE-2 cloudy column observations, *J. Geophys. Res.*, *108*(D24), 4762, doi:10.1029/2003JD003902.
- Nenes, A., P. Y. Chuang, R. C. Flagan, and J. H. Seinfeld (2001), A theoretical analysis of cloud condensation nucleus (CCN) instruments, *J. Geophys. Res.*, *106*, 3449–3474.
- Ovtchinnikov, M., and S. J. Ghan (2005), Parallel simulations of aerosol influence on clouds using cloud-resolving and single-column models, *J. Geophys. Res.*, *110*, D15S10, doi:10.1029/2004JD005088.
- Peng, Y., U. Lohmann, and R. Leitch (2005), Importance of vertical velocity variations in the cloud droplet nucleation process of marine stratus clouds, *J. Geophys. Res.*, *110*, D21213, doi:10.1029/2004JD004922.
- Penner, J. E., X. Dong, and Y. Chen (2004), Observational evidence of a change in radiative forcing due to the indirect aerosol effect, *Nature*, *427*, 231–233.
- Pitzer, K. S. (1973), Thermodynamics of electrolytes. I. Theoretical basis and general equations, *J. Phys. Chem.*, *77*, 268–277.
- Pitzer, K. S., and G. Mayorga (1973), Thermodynamics of electrolytes. II. Activity and osmotic coefficients for strong electrolytes with one or both ions univalent, *J. Phys. Chem.*, *77*, 2300–2308.
- Pruppacher, H. R., and J. D. Klett (1997), *Microphysics of Clouds and Precipitation*, Springer, New York.
- Rissman, T. A., T. M. VanReken, J. Wang, R. Gasparini, D. R. Collins, Y.-N. Lee, H. Jonsson, F. J. Brechtel, R. C. Flagan, and J. H. Seinfeld (2006), Characterization of cloud condensation nuclei (CCN) during the 2003 Atmospheric Radiation Measurement aerosol intensive operational period at the Southern Great Plains site in Oklahoma, *J. Geophys. Res.*, doi:10.1029/2004JD005695, in press.
- Schmid, B., et al. (2006), How well can we measure the vertical profile of aerosol extinction?, *J. Geophys. Res.*, doi:10.1029/2005JD005837, in press.
- Sheridan, P. J., D. J. Delene, and J. A. Ogren (2001), Four years of continuous surface aerosol measurements from the Department of Energy's Atmospheric Radiation Measurement Program Southern Great Plains Cloud and Radiation Testbed site, *J. Geophys. Res.*, *106*, 20,735–20,747.
- Snider, J. R., S. Guibert, J.-L. Brenguier, and J.-P. Putaud (2003), Aerosol activation in marine stratocumulus clouds: 2. Kohler and parcel theory closure studies, *J. Geophys. Res.*, *108*(D15), 8629, doi:10.1029/2002JD002692.
- Tang, I. N., and H. R. Munkelwitz (1994), Water activities, densities, and refractive indices of aqueous sulfates and sodium nitrate droplets of atmospheric importance, *J. Geophys. Res.*, *99*, 18,801–18,808.
- Turner, D. D., and J. Goldsmith (2005), The refurbishment and upgrade of the ARM Raman Lidar, paper presented at 15th ARM Science Team Meeting, U.S. Dep. of Energy, Daytona Beach, Fla. (Available at [http://www.arm.gov/publications/proceedings/conf15/extended\\_abs/turner\\_dd1.pdf](http://www.arm.gov/publications/proceedings/conf15/extended_abs/turner_dd1.pdf))
- Turner, D. D., R. A. Ferrare, L. A. Heilman, W. F. Feltz, and T. P. Tooman (2002), Automated retrievals of aerosol extinction coefficient from a Raman lidar, *J. Atmos. Oceanic Technol.*, *19*, 37–50.
- Wang, J., R. C. Flagan, and J. H. Seinfeld (2003), A differential mobility analyzer (DMA) system for submicron aerosol measurements at ambient relative humidity, *Aerosol Sci. Technol.*, *37*, 46–52.
- Yum, S. S., and J. G. Hudson (2002), Maritime/continental microphysical contrasts in stratus, *Tellus, Ser. B*, *54*, 61–73.
- R. Elleman, Department of Atmospheric Science, University of Washington, Seattle, WA 98195, USA.
- R. A. Ferrare, NASA Langley Research Center, Hampton, VA 23681-0001, USA.
- R. C. Flagan, T. A. Rissman, J. H. Seinfeld, and T. VanReken, California Institute of Technology, Pasadena, CA 91125, USA.
- C. Flynn, S. J. Ghan, and D. Turner, Pacific Northwest National Laboratory, Richland, WA 99352, USA. (steve.ghan@arm.gov)
- J. Hudson, Desert Research Institute, Reno, NV 89512, USA.
- H. H. Jonsson, Naval Postgraduate School, Monterey, CA 93943, USA.
- J. Ogren, NOAA Climate Monitoring and Diagnostics Laboratory, Boulder, CO 80303, USA.
- J. Wang, Brookhaven National Laboratory, Upton, NY 11973, USA.